

# COMPARISON OF CONVECTIVE OVERSHOOTING MODELS AND THEIR IMPACT ON ABUNDANCES FROM INTEGRATED LIGHT SPECTROSCOPY OF YOUNG (< 3 GYR) STAR CLUSTERS<sup>1</sup>

JANET E. COLUCCI

Department of Astronomy and Astrophysics, 1156 High Street, UCO/Lick Observatory,  
University of California, Santa Cruz, CA 95064; jcolucci@ucolick.org

AND

REBECCA A. BERNSTEIN

Department of Astronomy and Astrophysics, 1156 High Street, UCO/Lick Observatory,  
University of California, Santa Cruz, CA 95064; rab@ucolick.org

*Submitted to ApJ August 24, 2011, Accepted November 21, 2018*

## ABSTRACT

As part of an ongoing program to measure detailed chemical abundances in nearby galaxies, we use a sample of young to intermediate age clusters in the Large Magellanic Cloud with ages of 10 Myr to 2 Gyr to evaluate the effect of isochrone parameters, specifically core convective overshooting, on Fe abundance results from high resolution, integrated light spectroscopy. In this work we also obtain fiducial Fe abundances from high resolution spectroscopy of the cluster individual member stars. We compare the Fe abundance results for the individual stars to the results from isochrones and integrated light spectroscopy to determine whether isochrones with convective overshooting should be used in our integrated light analysis of young to intermediate age (10 Myr -3 Gyr) star clusters. We find that when using the isochrones from the Teramo group, we obtain more accurate results for young and intermediate age clusters over the entire age range when using isochrones without convective overshooting. While convective overshooting is not the only uncertain aspect of stellar evolution, it is one of the most readily parametrized ingredients in stellar evolution models, and thus important to evaluate for the specific models used in our integrated light analysis. This work demonstrates that our method for integrated light spectroscopy of star clusters can provide unique tests for future constraints on stellar evolution models of young and intermediate age clusters.

*Subject headings:* galaxies: individual (LMC) — galaxies: star clusters — galaxies: abundances — globular clusters: individual (NGC 1978, NGC 1866, NGC 1711, NGC 2100) — stars: abundances

## 1. INTRODUCTION

We are conducting a study of Large Magellanic Cloud (LMC) clusters in the young to intermediate age range with the ultimate goal of obtaining detailed abundances of over 20 elements from integrated light (IL), high resolution spectroscopy. Our method uses stellar evolution models and isochrones to create representative color magnitude diagrams (CMDs), with which to execute detailed spectral synthesis. To understand our accuracy we must evaluate to what extent uncertainties in stellar evolution modeling can affect our results. In Colucci et al. (2009) and Colucci et al. (2011) (hereafter C11), we evaluated relevant issues for old (>5 Gyr) clusters, mainly uncertainties in horizontal branch morphology and asymptotic giant branch stars. In this work, we address additional challenges in analysis of young and intermediate age clusters (age <3 Gyr), concentrating on the effects of core convective overshooting in the isochrones. While the inclusion of convective overshooting is not the only uncertainty in stellar models for young stars (for example, see Ventura & Castellani 2005), it is a key parameter causing significant differences in evolution of young stars; consequently stellar modeling groups do tabulate isochrone families with different values of convective overshooting.

Briefly, convective overshooting (C-OVER) refers to the treatment of convection at the border of stellar cores. Stars that are more massive than  $\sim 1.1 M_{\odot}$  are hot enough to develop a convective core during the main sequence, H-burning phase. Note that, because only relatively massive stars develop convective cores, the treatment of C-OVER is only important for star clusters that are younger than  $\sim 3$  Gyr. Historically, two types of treatments have been used in stellar evolution models to describe stars with convective stellar cores. The first, most simplistic model, uses the Schwarzschild criterion to treat convective instability. In this case there is a clean boundary at the edge of the convective stellar core, and the stellar properties (luminosity, lifetime, etc.) are determined by the input stellar physics. The second treatment parametrizes a certain amount of mechanical convective overshooting past the Schwarzschild core boundary. The addition of C-OVER into the stellar evolution models is physically motivated by the fact that fluid elements could maintain some velocity when moving past the Schwarzschild boundary, due to residual momentum or the star's rotational velocity (e.g. Meynet & Maeder 2000). In stellar evolution models, the empirical effect of including C-OVER is an increase in the size of the stellar core, which results in a higher stellar luminosity and a shorter stellar lifetime.

Observations of stellar clusters have been used to try to constrain the appropriateness and magnitude of C-

<sup>1</sup> This paper includes data gathered with the 6.5 meter Magellan Telescopes located at Las Campanas Observatory, Chile.

OVER that should be included in stellar evolution models. Because including C-OVER in the stellar models increases the luminosities of supergiant stars, which have ages of  $\sim 100$ 's of Myrs, C-OVER models in this age range will predict older ages for stellar clusters than models without C-OVER. This is visually apparent in Figure 1, where we show examples of Teramo (Pietrinferni et al. 2004) isochrones with and without C-OVER for ages of 0.1, 0.3, 1.0, and 2.0 Gyr, and metallicities of  $[\text{Fe}/\text{H}] = 0$  and  $[\text{Fe}/\text{H}] = -0.35$ . For ages of 0.1 and 0.3 Gyr, the turnoff stars and blue loop supergiants have brighter magnitudes when C-OVER is included (shown by the pink dashed lines). Figure 1 also demonstrates that the differences in the giant populations of the different sets of isochrones become smaller as the age of the isochrones increases. For ages of  $\sim 2$  Gyr, the giant populations are very similar; only a small difference in the turnoff morphologies is evident. Finally, Figure 1 shows that, with the exception of the 2 Gyr case, the differences between isochrones with and without C-OVER are greater for the lower metallicity of  $[\text{Fe}/\text{H}] = -0.35$ , which is roughly the present day metallicity of the LMC, than they are for higher metallicities of  $[\text{Fe}/\text{H}] = 0$ .

While C-OVER was introduced into stellar evolution models to reproduce observations of stars in young stellar clusters, the appropriateness and magnitude of C-OVER that is required is still under debate. For ages of  $\sim 150$  Myr, where differences are most dramatic for supergiant stars, various authors have tried to use the CMD of NGC 1866 to constrain the physics of the stellar evolution models. Different authors have reached different conclusions, and the results appear to be dependent on the set of stellar models that are used. For example, using a ground based CMD and FRANEC (Straniero et al. 1997) models, Testa et al. (1999) determined that C-OVER was not required to match observations of NGC 1866. On the other hand, Barmina et al. (2002), using the same dataset as Testa et al. (1999), found that when using the Padova (Girardi et al. 2000) models, it is necessary to include C-OVER in order to reproduce the observations. Later, Brocato et al. (2003) and Brocato et al. (2004) used a Hubble Space Telescope (HST) WFPC2 CMD of NGC 1866 to determine the best fitting degree of C-OVER with higher quality data. They found that C-OVER was not required to fit the observations using the Pisa (Castellani et al. 2003) stellar models, but that when Padova models are used, including C-OVER still provides a better fit, as found using the ground based CMDs. Unfortunately, to the best of our knowledge, the Teramo (Pietrinferni et al. 2004) models with and without C-OVER that we use in our IL analysis have not been compared to observations of NGC 1866.

For clusters with older ages ( $\sim 2$  Gyrs), high precision HST ACS photometry was analyzed by Mucciarelli et al. (2007a) and Mucciarelli et al. (2007b) for the LMC clusters NGC 1978 and NGC 1783. These authors tested stellar evolution models from several different groups, including the Teramo isochrones, and concentrated on the turnoff regions of the clusters, where differences are most visible in this age range. After testing the Teramo, Pisa, and Padova models, the authors found that some amount of C-OVER is required to match the turnoff region, regardless of which set of models were used.

### 1.1. Background: The Impact on High Resolution Integrated Light Spectroscopy

As described above, we use a grid of isochrones when measuring abundances with our high resolution, integrated light spectra abundance analysis method (see Bernstein & McWilliam 2002; McWilliam & Bernstein 2008; Cameron 2009; Colucci 2010; Colucci et al. 2009, 2011, for full details). For long-term consistency, it is crucial that we choose a single group of isochrones to use in all of our analyses. We have selected those of the Teramo group (Pietrinferni et al. 2004, 2006), because they provide a wide range of ages, metallicities and two levels of  $\alpha$ -enhancement. The Teramo isochrones are also tabulated with two values of C-OVER: no C-OVER (listed as canonical) and with moderate C-OVER (listed as non-canonical).

Our initial work concerned typical old globular clusters with ages  $> 5$  Gyr, which are not sensitive to inclusion of C-OVER because the stars in old clusters are not massive enough to have convective cores. However, in C11 we extended our method to young clusters in the LMC, and it became clear that our results for the youngest clusters (ages  $< 1$  Gyr) could be significantly affected by the choice of C-OVER. In C11, we chose to adopt the Teramo isochrones with C-OVER included, because Mucciarelli et al. (2007a) determined that these isochrones were a better match to the CMD of NGC 1978, a cluster that is also in our sample, than isochrones without C-OVER. Unfortunately, there was no consensus in the literature for the use of C-OVER for clusters over the entire age range of the young clusters in our sample (10 Myr to 2 Gyr). While several authors concluded that no C-OVER was needed in order to match observations of NGC 1866 (age 150 Myr), none of these authors tested isochrones from the Teramo group. Note that this result is at odds with the results for NGC 1978 (age 2 Gyr). We mentioned above that because C-OVER is not the only uncertainty in stellar evolution physics, conclusions regarding the need for C-OVER are dependent on the set of models being used. Therefore, in order for us to determine the “right” set of models to use in our new IL analysis method *over the entire cluster age range* we have to determine which set of models produces abundances for our sample of local clusters that are closest to the abundances for these clusters determined by other well-established methods.

In C11, initial tests of isochrones with and without C-OVER for clusters with ages of 2 Gyr showed that the differences were smaller than the statistical uncertainties of the solutions. However, results for clusters with ages  $< 1$  Gyr were not always in agreement with the few results available in the literature. Unfortunately, more than half of the young clusters in our sample had no previous abundance measurements from high resolution abundance analysis of individual stars. Moreover, because individual star analyses performed by different authors do not agree to better than  $\sim 0.10 - 0.15$  dex (Gratton et al. 2004; Cameron 2009), we cannot be certain which differences can be attributed to isochrone physics, and which are due to systematic offsets between different abundance analysis techniques. We have therefore completed our own analysis of individual stars in the young clusters in our sample, to obtain abundances us-

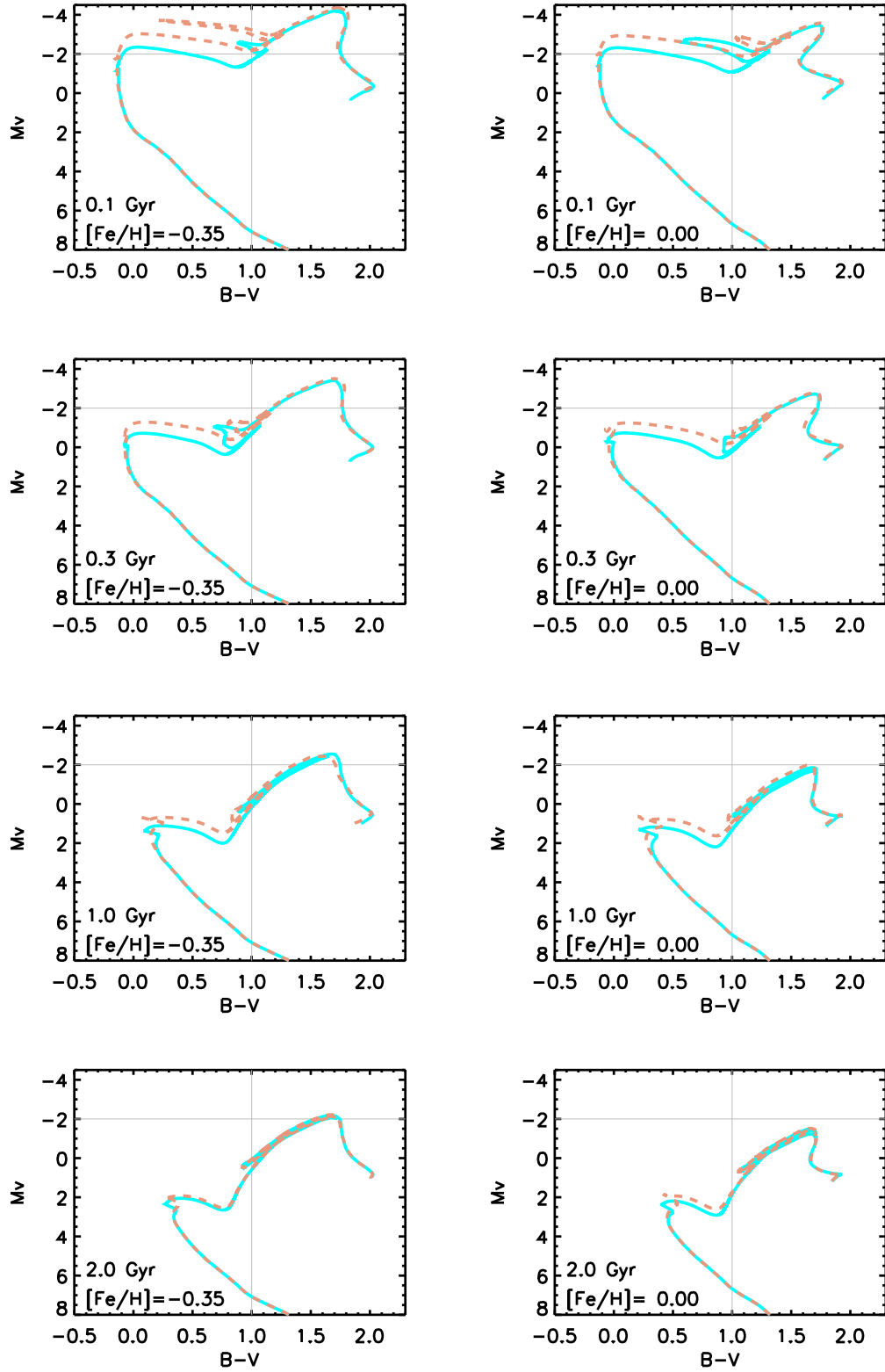


FIG. 1.— Comparison of Teramo isochrones with no C-OVER (cyan) and with C-OVER (pink) for ages of 0.1 to 2 Gyr and metallicities of  $[\text{Fe}/\text{H}] = -0.35$  and  $[\text{Fe}/\text{H}] = 0.00$ , as shown. Gray lines are shown to guide the eye. For ages  $< 1$  Gyr the inclusion of C-OVER results in large differences in the supergiant populations, while for ages  $> 1$  Gyr there are only subtle differences in the turnoff morphology. The differences between the models are typically larger at lower metallicity.

ing identical line lists, stellar atmospheres, and spectral synthesis codes as in our IL spectra analysis. We identify the most accurate set of isochrones as those that produce the Fe abundances closest to the Fe abundances that we measure for the individual stars analyzed in this work.

We note that in the literature convective overshooting has been extensively studied using a much larger sample of clusters than we describe here, including many nearby open clusters in the Milky Way. We emphasize that our principle intent is to specifically evaluate the most appropriate set of Teramo isochrones for use in our high resolution integrated light spectra technique. In this regard, we refrain from any analysis or comparison of Teramo isochrones to resolved photometric color magnitude diagrams of the LMC clusters in our sample. While such an analysis would be very interesting to compare to the results here, it is beyond the scope of the present spectroscopic analysis and does not address our primary goal of determining which Teramo isochrones result in integrated light Fe abundances that most closely match fiducial Fe abundances from individual stars.

This paper is organized as follows: in §2 we describe the stellar and cluster targets and data reduction techniques. In §3 we present the high resolution Fe abundance analysis for the individual stars in the LMC clusters, and review the analysis for the integrated light spectra of the clusters originally presented in C11. In §4 we present the results, discuss some of the sources of the differences in results when using different values of C-OVER in the IL analysis, and identify the set of isochrones for which the most accurate Fe abundances are obtained.

## 2. OBSERVATIONS AND DATA REDUCTION

### 2.1. Cluster Integrated Light

Our integrated light spectra of NGC 1978, NGC 1866, NGC 1711, and NGC 2100 were obtained using the echelle spectrograph on the 2.5 m du Pont telescope at Las Campanas during dark time in 2000 December and 2001 January. The wavelength coverage is approximately 3700–7800 Å.

Integrated light spectra were obtained by scanning a  $12 \times 12$  arcsec<sup>2</sup> or  $8 \times 8$  arcsec<sup>2</sup> region of each cluster core (McWilliam & Bernstein 2008). These spectra were reduced with standard IRAF<sup>2</sup> routines, combined with the scattered-light subtraction described in McWilliam & Bernstein (2008). Complete details on the cluster integrated light observations and reductions can be found in McWilliam & Bernstein (2008) and C11.

### 2.2. Cluster Stars

Stars were selected from the catalogs of Will et al. (1995), Brocato et al. (1989), Sagar et al. (1991), and Robertson (1974) for NGC 1978, NGC 1866, NGC 1711, and NGC 2100, respectively. Information on the target stars, exposure times, and approximate signal-to-noise (S/N) ratios are given in Table 1.

The spectra of individual stars in the LMC clusters were obtained with the MIKE double echelle spectrograph (Bernstein et al. 2003) on the Magellan Clay Telescope during three different observing runs in 2003 and

2004. The setup of the spectrograph changed between the runs, which resulted in different wavelength coverages for the individual runs. However, we primarily use lines with wavelengths between 4500–7500 Å (red side only) in our analysis, which is a region in common to all three runs. The data taken in 2003 January used a  $0.7'' \times 5''$  slit and  $4 \times 2$  on chip binning. The data taken in 2003 November used a  $0.5'' \times 5''$  slit and  $3 \times 1$  on chip binning, while the data from 2004 October used a  $0.7'' \times 5''$  slit and  $3 \times 2$  on chip binning. The stellar spectra were reduced using the MIKE Redux<sup>3</sup> pipeline (Bernstein et al. 2012, in preparation), which includes a heliocentric velocity correction.

Radial velocities of the stars are measured with the analysis code GETJOB (see §3.1). The radial velocities ( $v_r$ ) are calculated by determining velocity offsets in the spectra from a list of input strong lines. Our averaged values are in good agreement with values in the literature. For NGC 1978 we measure  $v_r = 291.5 \pm 2.0$  km s<sup>-1</sup>, which agrees with the values of Hill et al. (2000), Mucciarelli et al. (2008), and Olszewski et al. (1991) of  $293.5 \pm 1.8$ ,  $293.1 \pm 1.5$ , and  $292.4 \pm 0.4$  km s<sup>-1</sup>, respectively. For NGC 1866 we measure  $v_r = 301.5 \pm 1.1$  km s<sup>-1</sup>, which agrees well with the values of Hill et al. (2000) and Mucciarelli et al. (2010) who found  $299.8 \pm 1.4$  and  $298.5 \pm 1.5$  km s<sup>-1</sup>. We measure  $v_r = 244.2 \pm 2.8$  km s<sup>-1</sup> for NGC 1711, which is within  $2 \sigma$  of the value measured by Freeman et al. (1983) of  $230 \pm 9$  km s<sup>-1</sup>. Similarly, our measurement of  $v_r = 247.6 \pm 5.7$  km s<sup>-1</sup> for NGC 2100 is within  $2 \sigma$  of the value of Jasniewicz & Thevenin (1994) of  $262.5 \pm 6.45$  km s<sup>-1</sup>.

## 3. ABUNDANCE ANALYSIS

Where possible, we have used identical analysis techniques for both the IL analysis of clusters and for the individual member stars. In §3.1 we describe the line lists and equivalent width measurements that both analyses have in common. In §3.2 we briefly review the IL analysis of C11, and in §3.3 we describe the new analysis of individual stars performed in this work.

### 3.1. EWs and Line Lists

As in our previous work (e.g. C11, and references therein), we use the semi-automated program GETJOB (McWilliam et al. 1995) to measure absorption line equivalent widths (EWs) for individual lines in both the cluster IL and stellar spectra in a consistent way. Low order polynomials are interactively fit to continuum regions for each spectral order, and line profiles are fit with single, double, or triple Gaussians as needed, depending on the presence of small line blends. Line lists and log  $gf$  values are taken from C11 and references therein. We only analyze Fe lines with EWs < 150 mÅ in order to minimize line saturation effects. Fe abundances are calculated under the assumption of local thermodynamic equilibrium (LTE). The lines and EWs measured in the individual stars are listed in Table 2.

### 3.2. Cluster Integrated Light

In C11 we presented a detailed analysis of the integrated light [Fe/H] and age solutions for each LMC cluster in our sample using Teramo isochrones with C-OVER

<sup>2</sup> IRAF is distributed by the National Optical Astronomy Observatories, which are operated by the Association of Universities for Research in Astronomy, Inc., under cooperative agreement with the National Science Foundation.

<sup>3</sup> <http://www.ucolick.org/~xavier/IDL/index.html>

included. In this work, we perform an identical analysis but use the Teramo isochrones without C-OVER, as discussed in §1. We summarize this analysis below.

We create synthetic CMDs for the available range of age and metallicity of the Teramo isochrones, and divide each CMD into  $\sim 25$  equal flux boxes containing stars of similar properties. The properties of a flux-weighted “average” star for each box are used in the IL EW synthesis, which we perform with ILABUNDS (McWilliam & Bernstein 2008). ILABUNDS employs the 2010 version of the spectral synthesis code MOOG (Snedden 1973). We use the ODFNEW model stellar atmospheres of Kurucz<sup>4</sup> (e.g. Castelli & Kurucz 2004) for all abundance analysis. We choose the ODFNEW atmospheres instead of the AODFNEW atmospheres because we have determined that the clusters are not significantly  $\alpha$ -enhanced, as reported in Colucci et al. (2012).

To begin the analysis of any cluster, we calculate a mean [Fe/H] abundance from all available Fe I lines for the large grid of synthetic CMDs. We note that because we measure far fewer Fe II lines than Fe I lines in the cluster IL spectra, and because of uncertainties in the relationship between neutral and ionized solutions, we do not use Fe II lines to constrain the best-fitting CMD. We next use the quality of the Fe I abundance solution to constrain the best-fitting age and abundance for each cluster. Specifically, we determine the best age and abundance using Fe line diagnostics (McWilliam & Bernstein 2008; Colucci et al. 2009, 2011). These diagnostics, also used in the standard stellar abundance analysis below, relate to the quality of the [Fe/H] solutions. In particular, a stable [Fe/H] solution should not depend on the parameters of individual lines (excitation potentials, wavelengths, or reduced EWs<sup>5</sup>), and the standard deviation of the [Fe/H] solution should be small.

Finally, we can improve our solutions by allowing for statistically incomplete sampling of the cluster CMDs (C11). It is especially important to allow for statistical variations for clusters with ages under  $\sim 2$  Gyrs, because clusters with these ages are rapidly evolving, and in the case of our sample, they are less luminous and less massive than typical Milky Way GCs, and therefore the most likely to suffer from stochastic effects. In order to quantify this uncertainty we use a Monte Carlo technique to statistically populate the cluster initial mass functions (IMFs) with discrete numbers of stars, resulting in many possible realizations of each cluster. As demonstrated in C11, the best statistical realizations of each cluster can be identified using the Fe line diagnostics.

Here, we briefly summarize the effect that the Monte Carlo tests have on the derived [Fe/H] and age of each cluster. For NGC 1718 the [Fe/H] decreases marginally from -0.67 to -0.70, and the uncertainty due to the age solution is unchanged, at 0.03. For NGC 1978, we find that allowing for stochastic sampling decreases the derived [Fe/H] from -0.48 to -0.54, and increases the uncertainty due to the age from 0.05 to 0.18. For NGC 1866, the [Fe/H] abundance is unchanged, but the uncertainty due to the age increases from 0.16 to 0.20. For NGC 1711, both the derived [Fe/H] and uncertainty due

to the age are unchanged. As in C11, we are only able to derive a solution for NGC 2100 by allowing for statistical fluctuations, so there is no added uncertainty.

In summary, the most self-consistent age and [Fe/H] solutions that we have determined for each cluster are listed in Table 3. In columns 2 and 3, we show the best-fitting age and [Fe/H] solutions determined for isochrones with C-OVER in C11 and in columns 4 and 5 we show the best-fitting age and [Fe/H] solutions determined using isochrones without C-OVER from this work. We note that we include results for the IL abundances of NGC 1718 in Table 3, but we do not have a sample of individual stars in this cluster and so the IL results are not used for the IL and stellar direct comparison in §4. As already discussed, the measurement of the ages and metallicities from the IL spectra was explained in detail in C11, and is accompanied by an in depth comparison of the derived ages and [Fe/H] to values in the literature. We note that the ages derived in this work using isochrones without C-OVER are consistent with the conclusions of C11, so we do not repeat that discussion here.

### 3.3. Cluster Stars

To begin the analysis of the individual stars, we determined initial atmospheric parameters for the cluster stars using the photometric data described in §2.2. The reddening corrected absolute V magnitudes and  $B - V$  colors that we used are listed in Table 4. With these colors we determined stellar temperatures using the empirical  $(B - V) - T_{eff}$  calibration of Alonso et al. (1999). Surface gravities are calculated according to the equation

$$\log g = \log g_{\odot} + \log M/M_{\odot} - \log L/L_{\odot} + 4 \log T_{eff}/T_{eff\odot} \quad (1)$$

assuming  $T_{eff\odot} = 5777$  K and  $\log g_{\odot} = 4.44$ . Bolometric corrections are interpolated from the grids of Kurucz,<sup>6</sup> with  $M_{bol\odot} = 4.74$ . We have assumed stellar masses of  $1.8 M_{\odot}$  for NGC 1978,  $4.5 M_{\odot}$  for NGC 1866, and  $8.5 M_{\odot}$  for NGC 1711 and NGC 2100. These masses were determined using the turnoff masses of Teramo isochrones with appropriate ages and metallicities for each cluster. Stellar luminosities were calculated using the distance moduli and  $E(B - V)$  values listed in Table 1. Initial microturbulent velocities ( $\xi$ ) were calculated as for our IL analysis (see McWilliam & Bernstein 2008), by assuming a linear relationship between the  $\xi$  of the Sun and Arcturus. As in the cluster IL analysis, we use the Kurucz ODFNEW stellar atmospheres and the most recent (2010) version of MOOG (Snedden 1973). We use the ODFNEW atmospheres instead of the AODFNEW ones because we have determined that the stars are not significantly enhanced in  $\alpha$ -elements, as presented in Colucci et al. (2012).

The initial values that we adopt for stellar mass, reddening, and microturbulence are subject to the usual observational uncertainties; we therefore constrain these parameters spectroscopically, as is standard in abundance analysis of individual stars. We first iteratively adjust the effective temperature and microturbulence to simultaneously obtain a solution with no dependence of Fe I abundance on the excitation potential (EP) or reduced equivalent widths of the lines. On average, we

<sup>4</sup> The models are available from R. L. Kurucz’s Website at <http://kurucz.harvard.edu/grids.html>

<sup>5</sup> Reduced EW  $\equiv \log(EW / \lambda)$

<sup>6</sup> Available from <http://kurucz.harvard.edu/grids.html>

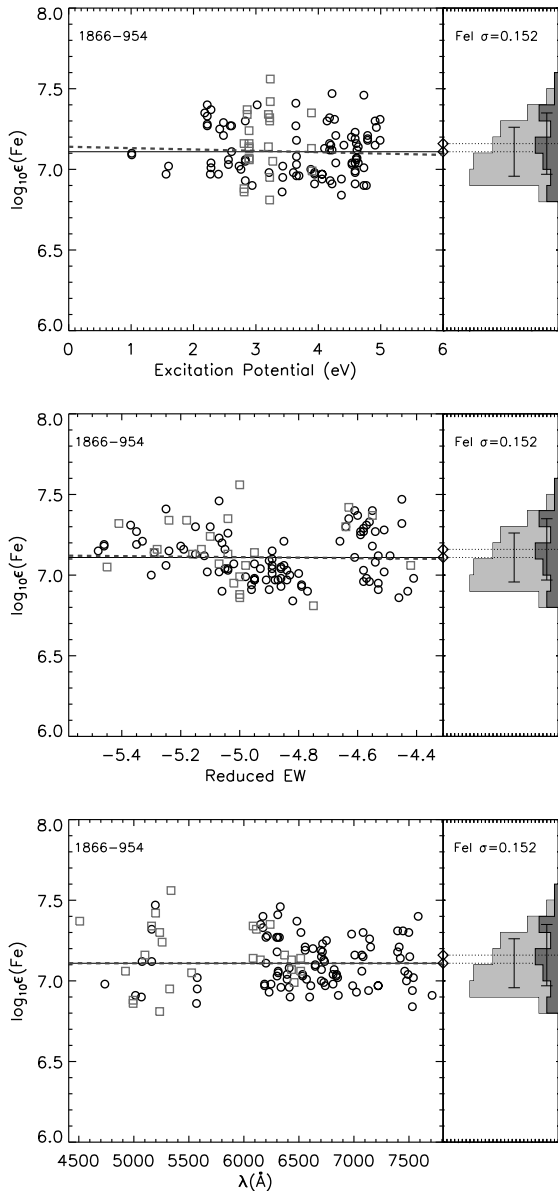


FIG. 2.— Examples of Fe abundance diagnostic plots, shown for star 954 in NGC 1866. Fe I and Fe II lines are indicated by circles and squares, respectively. Solid lines show the mean abundance of the Fe I lines, which was used to constrain the stellar parameters. Dashed lines show a linear least squares fit to the abundance of Fe I lines with EP, reduced EW, and wavelength, respectively.

find that the photometrically derived  $T_{eff}$  and  $\xi$  values need to be adjusted by less than 100 K and  $0.3 \text{ km s}^{-1}$  to eliminate the dependence of abundance on EP and reduced EW, respectively. This is independent verification that the microturbulence law that we employ in our IL analysis provides reasonably accurate values for younger stars. However, in the case of two very young supergiants, 2100-c12 and 2100-b22, our initial values for  $\xi$  were significantly underestimated. In these cases, we had to adjust the  $\xi$  by about  $1.5 \text{ km s}^{-1}$ , to  $\xi=3.3 \text{ km s}^{-1}$ , in order to eliminate the trend in Fe I abundance with reduced EW. Because such young supergiants are generally found to have  $\xi \sim 3 \text{ km s}^{-1}$  (e.g. Hill 1999), we believe that these spectroscopically determined values are reasonable.

In almost all cases, we find that the spectroscopically determined  $T_{eff}$  and  $\xi$  also result in solutions closer to ionization equilibrium, reducing the difference between abundances derived from Fe I and Fe II lines. This improvement is shown in Table 5, where we tabulate Fe I and Fe II abundance results for our photometrically and spectroscopically determined parameters.

In two cases, 1978-730 and 1866-954, we also adjust the surface gravity,  $\log g$ , to force ionization equilibrium for the Fe lines. In these two cases we find that adjusting the  $\log g$  not only results in a solution where neutral and ionized Fe are closer to ionization equilibrium, but also neutral and ionized Ti, Y, and Sc are closer to equilibrium. In two other cases, 1866-1653 and 1711-988, there are also large differences in abundance derived from Fe I and Fe II lines, but we do not adjust the  $\log g$  in these cases because we are unable to find a set of stellar parameters that simultaneously improve Fe, Ti, Y and Sc ionization equilibrium. 1866-1653 also has a particularly high line-to-line scatter for Fe II of  $\sigma_{\text{FeII}}=0.40$ . In this case we keep the initial  $\log g$  value because of the uncertainty of the Fe II abundance.

Our final adopted stellar parameters and Fe abundance results are listed in Table 4. Our final model atmospheres are adjusted so that the input  $[M/H]$  is identical to the derived Fe I abundance. As an example of one of our solutions, we show the dependence of Fe abundance on EP, reduced EW, and wavelength in Figure 2 for the star 954 in NGC 1866. Little or no trend in the Fe abundance with wavelength indicates that our continuum placement between orders is accurate and consistent.

We emphasize again that while the initial physical parameters used in the analysis of the spectra of stars (mass, effective temperature, and microturbulence) are drawn from the literature and those values can be affected by uncertainties such as reddening and photometric errors, the final values used for these parameters are spectroscopically constrained based on consistency in the iron abundance derived for lines over the full spectrum (i.e. with a wide range in wavelength, excitation potential, and reduced equivalent width). The uncertainties in the initial values are therefore irrelevant as they are merely initial guesses. What is relevant is the sensitivity of our solution to small errors in these iteratively-derived values. We therefore determine the systematic uncertainties resulting from our choice of atmospheric parameters explicitly by adjusting one parameter at a time and noting the impact on the resulting abundance. The results

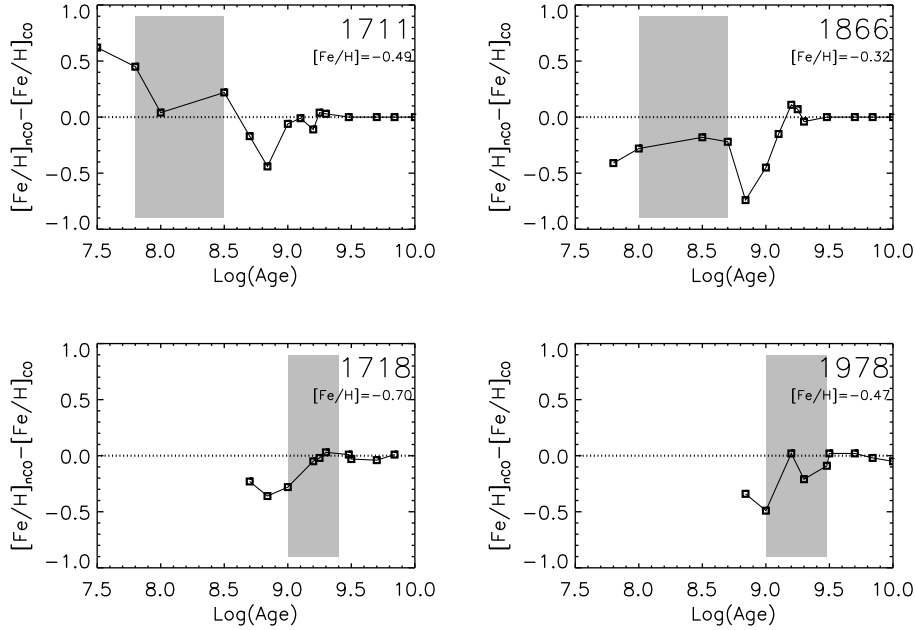


FIG. 3.— Difference in derived  $[\text{Fe}/\text{H}]$  for isochrones with no C-OVER ( $[\text{Fe}/\text{H}]_{\text{inCO}}$ ) (from this work) and with C-OVER ( $[\text{Fe}/\text{H}]_{\text{CO}}$ ) (from C11) for IL analysis of NGC 1711, NGC 1866, NGC 1718 and NGC 1978. The age range with the best solutions in our IL analysis is highlighted. Note that NGC 2100 is not included in this figure because the solutions between 0.06 and 1 Gyr do not converge due to this cluster’s young age (see C11, for more details).

are shown in Table 6, where we list the uncertainty in the derived  $[\text{Fe}/\text{H}]$  for each star for an uncertainty in  $T_{\text{eff}}=+150$  K,  $\log g=-0.5$  dex,  $\xi=+0.3$  km s $^{-1}$ , and  $[\text{M}/\text{H}]=+0.3$  dex. The total systematic error is typically between 0.1 and 0.2 dex.

To compare to our IL results, we average the  $[\text{Fe}/\text{H}]$  results for the individual stars. For NGC 2100, we find that the star c2 has a derived  $[\text{Fe}/\text{H}]$  that is  $\sim 0.4$  dex more metal rich than the other two stars. The three stars have a spread in radial velocity of 11 km s $^{-1}$ , with c2 having the lowest velocity, so it is possible that c2 is not actually a cluster member. However the mean radial velocity for LMC field stars is most likely to be higher than the radial velocity for NGC 2100, not lower. This star is also bluer and more luminous than the other two stars, so the stellar parameters may be more uncertain because it is in a different evolutionary stage. To be conservative, 2100-c2 is left out of the mean for the cluster. The final mean  $[\text{Fe}/\text{H}]$  values are listed in Table 7, along with previous abundance measurements by other authors from high resolution spectroscopy of individual stars. There are no previous measurements of the Fe abundance of NGC 1711 from high resolution spectroscopy, so we list an estimate for the  $[\text{Fe}/\text{H}]$  measured from Strömgren photometry by Dirsch et al. (2000) for comparison. We find that our  $[\text{Fe}/\text{H}]$  results agree within the uncertainties with the results found by other authors to  $<0.10$  dex, with the exception of the  $[\text{Fe}/\text{H}]$  measured by Hill et al. (2000) for NGC 1978. Our result for NGC 1978 does however agree with the measurement of Mucciarelli et al. (2008) who had a much larger sample of stars than Hill et al. (2000). We also note that Olszewski et al. (1991) found a similar  $[\text{Fe}/\text{H}]$  to ours for NGC 1978 using low resolution calcium triplet spectroscopy. We conclude that these comparisons demonstrate that our stellar abundance analysis techniques are consistent with previous works.

#### 4. RESULTS

First we examine the general trends in the IL abundance results for the isochrones with and without C-OVER. When we determine the best-fitting CMD in the IL analysis, we begin by identifying one CMD for each age in our grid that has a self-consistent  $[\text{Fe}/\text{H}]$  solution. We define self-consistent solutions as those where the derived  $[\text{Fe}/\text{H}]$  from the Fe I lines is the same as the  $[\text{Fe}/\text{H}]$  of the isochrone used to create the CMD. We then identify the age range of the CMDs that produces the most stable  $[\text{Fe}/\text{H}]$  solution overall.

In comparing our results for isochrones with and without C-OVER, we can first look at how the self-consistent  $[\text{Fe}/\text{H}]$  solution changes as a function of the age of the CMD. Figure 3 shows this  $[\text{Fe}/\text{H}]$  difference for four clusters: NGC 1711, NGC 1866, NGC 1718, and NGC 1978. Note that we can evaluate the behavior of the solutions with and without C-OVER for NGC 1718, but that without a sample of individual stars we cannot evaluate the agreement with our own fiducial Fe abundances. In Figure 3, the region where the best age solutions are found is highlighted in each panel. It is clear from this figure that the clusters that are most affected by C-OVER are those younger than  $\sim 1$  Gyr. As expected, we also find that the derived  $[\text{Fe}/\text{H}]$  for each cluster is unchanged when using the isochrones without C-OVER when isochrones older than  $\sim 2.5$  Gyr ( $\log(\text{Age})=9.40$ ) are used, because there are no stars with masses  $\gtrsim 1.1 M_{\odot}$  present (see §1).

It is also interesting to note that the abundance is sensitive to the amount of C-OVER because 90% of the flux in a 100 Myr cluster, such as NGC 1866, is in the supergiant stars. This sensitivity was also illustrated in C11 where we showed that the Fe lines are extremely sensitive to the color or temperature of the supergiant stars. To further illustrate the impact of these young stars, in Figure 4, we show the contribution of the in-

dividual synthetic CMD boxes to the IL EW for a single Fe line for both  $[\text{Fe}/\text{H}] = 0$  and  $[\text{Fe}/\text{H}] = -0.3$  for the two sets of isochrones. Note that the best solution for NGC 1866 is  $[\text{Fe}/\text{H}] = -0.3$  without C-OVER, and  $[\text{Fe}/\text{H}] = 0$  with C-OVER, resulting from the differences in the supergiant populations. In Figure 4, the left panels demonstrate that almost the entire EW comes from the supergiants, while the right panels show that the CMDs differ most in the color of the supergiants. In particular, the  $[\text{Fe}/\text{H}] = -0.35$  isochrone with C-OVER has bluer supergiants than the isochrone with  $[\text{Fe}/\text{H}] = -0.35$  and no C-OVER. Note that only the latter provides a self-consistent  $[\text{Fe}/\text{H}]$  solution by our criterion discussed above.

Our final age and  $[\text{Fe}/\text{H}]$  solutions for isochrones with and without C-OVER are listed in Table 3. We find that the new IL results using isochrones without C-OVER show complex behavior when compared to the results obtained using isochrones with C-OVER. In other words, there is no constant offset that can be applied to the whole sample of clusters, because the new analysis results in higher  $[\text{Fe}/\text{H}]$  for NGC 1978, and NGC 1711, but lower  $[\text{Fe}/\text{H}]$  for NGC 1718 and NGC 1866. As already mentioned, the differences tend to get larger as the age of the cluster decreases. This means that the unpredictability in the magnitude and direction of the offset is likely due to the fact that the properties of the giant stars are so susceptible to stochastic effects.

We can now use our stellar results to evaluate the accuracy of the isochrones as discussed in §1. Comparing the results listed in Tables 3 and 7, we find that the isochrones with no C-OVER, labeled “canonical” by the Teramo group, more closely match the results we obtain from the individual stars. This is also clear from Figure 5, where we plot the results using isochrones with and without C-OVER against the abundance from individual stars. The bottom panel of Figure 5 shows the difference between the isochrone results and the individual star results. The statistical scatter of the residuals for the isochrones without C-OVER, which are plotted as black circles, is 0.24 dex, while the scatter of the residuals for the isochrones with C-OVER, plotted as cyan squares, is much larger, at 0.40 dex.

Figure 5 also shows that the largest difference in abundance determined from IL spectra is for the cluster with the highest  $[\text{Fe}/\text{H}]$ , which is the youngest cluster, NGC 2100. We note that our IL result for this cluster is the most uncertain, as it is at the youngest limit of what we can analyze using our current technique. In C11, we reported a lower limit for the  $[\text{Fe}/\text{H}]$  of NGC 2100, but it is obvious from this work that the cluster is more metal-poor than our limit, and perhaps an upper limit would have been more appropriate. We reported a lower limit because, in general, if the age of the cluster is younger than the isochrone, we would underestimate the abundance because the stellar temperatures would be lower in our model than in reality. However, in the case of very young clusters, age  $< 50$  Myr, the stochastic properties of the supergiants can make the behavior unpredictable. Therefore, we quote a final  $[\text{Fe}/\text{H}]$  for NGC 2100 with higher uncertainties ( $-0.4 < [\text{Fe}/\text{H}] < +0.03$ ) rather than a limit. We note that while the  $[\text{Fe}/\text{H}]$  for NGC 2100 is uncertain, the abundance ratios for all other elements are well constrained. In Colucci et al. (2012),

we discuss in more detail the agreement found by comparison of the abundance ratios obtained with IL analysis and individual stars.

It is interesting that Mucciarelli et al. (2008) find that Teramo isochrones with some degree of C-OVER are needed to match the turnoff region of the CMD of NGC 1978, and that we find that isochrones without C-OVER produce a more accurate  $[\text{Fe}/\text{H}]$  for this cluster in our IL analysis. As we have emphasized already, it is not our intent in this work to use our IL spectroscopy results to calculate the appropriate magnitude of C-OVER that should be in stellar evolution models, or to comment on how the Teramo isochrones fit the observed CMDs of the clusters we have analyzed. As inferred for the youngest clusters, it is likely that differences in the most luminous RGB and AGB stars in the isochrones are the reason that there is a difference in the derived  $[\text{Fe}/\text{H}]$ , and that when averaged and flux weighted the isochrones without C-OVER more closely match the real stellar populations in this cluster.

In conclusion, because clusters younger than 1 Gyr are most susceptible to stochastic stellar population effects, the abundance solutions for those clusters will be the most sensitive to including C-OVER in the CMDs. This is because the supergiants, whose properties can change substantially when using C-OVER or not, have a strong influence on the solution, and therefore determine how much the C-OVER parametrization will affect the results. Indeed, for clusters close to 0.05 Gyrs, the uncertainties in age and abundance determined by any method become much unavoidably impacted by both the stochastic effects of catching stars in the supergiant phases and the fundamental uncertainties in the simple stellar population (SSP) modeling. We do not find a predictable offset in the solutions obtained without C-OVER; however we do find that smaller scatter is obtained in the comparison of abundances obtained from stars and integrated light when C-OVER is omitted from the models. Therefore, for our IL abundance analysis purposes, the Teramo isochrones without C-OVER produce the most accurate  $[\text{Fe}/\text{H}]$  solutions. More generally, in this and our companion papers, we find that measurements of age and abundance in young clusters should include uncertainties associated with the stochastic variations in supergiant population during any given observation, and also the uncertainties in the SSP models, of which C-OVER is one important consideration.

## 5. SUMMARY AND CONCLUSIONS

We have performed high resolution Fe abundance analysis of individual stars in four LMC clusters in order to obtain fiducial Fe abundances in these clusters for comparison to Fe abundances that we measure using our high resolution integrated light spectra abundance analysis. Our primary goal in this work is to determine the most appropriate convective overshooting parameter in the Teramo isochrone set for our abundance analysis. From these comparisons we conclude that Teramo isochrones without convective overshooting result in Fe abundances that most closely match the results from individual stars for clusters with ages between 0.05 Gyr and 3 Gyr. In a separate paper, we present abundances for over 20 additional elements that are measured in the cluster IL spectra, as well as in the spectra of the indi-

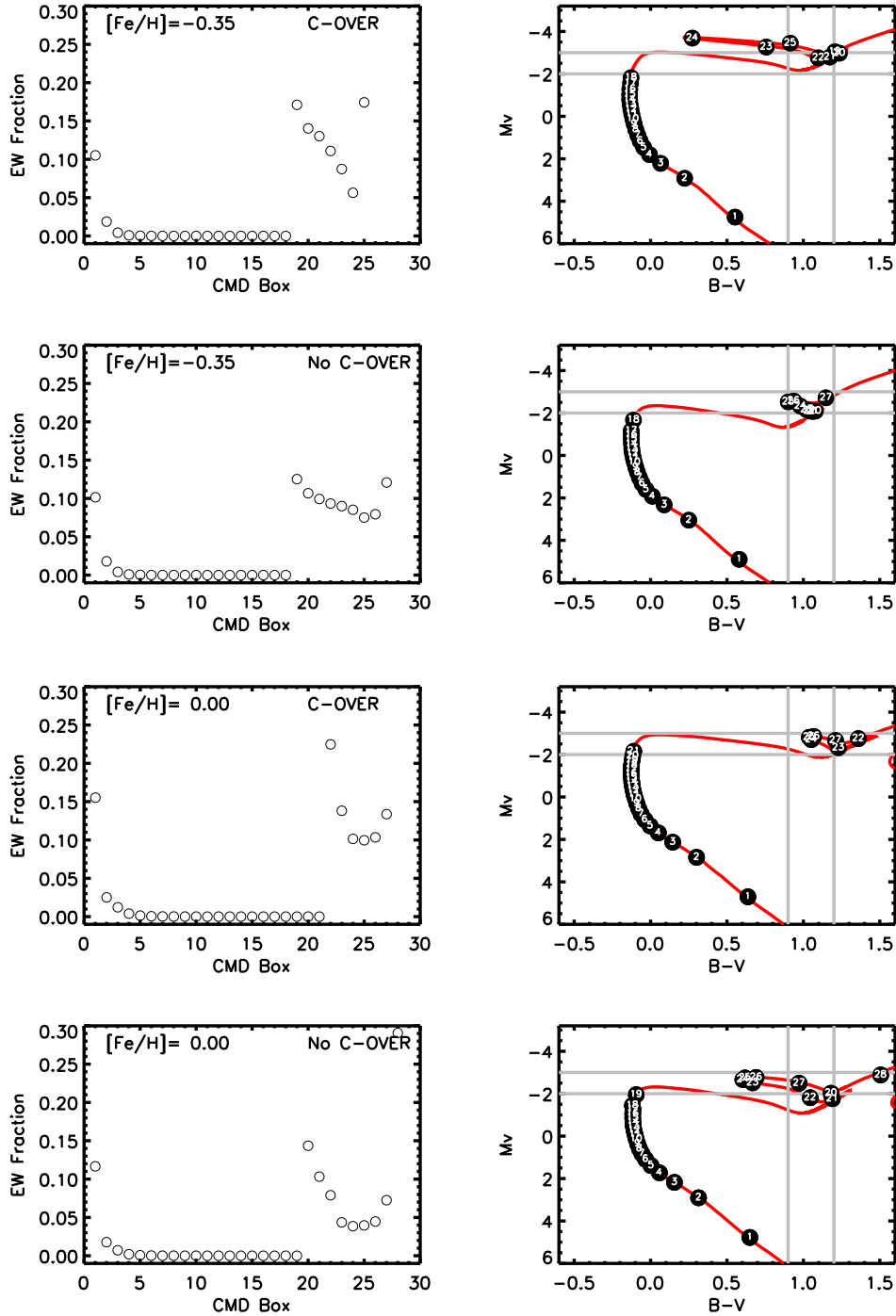


FIG. 4.— Left panels show the contribution of individual synthetic CMD boxes to the integrated light EW of the Fe I 6393 Å line (EP=2.43 eV), when different isochrones are used in constructing the CMDs. Right panels show the original isochrones in red, and the corresponding CMD boxes from the left panels in black. Gray lines are shown to guide the eye to the position of the supergiant CMD boxes. All isochrones have an age of 0.1 Gyrs. Isochrones in the top four plots have  $[\text{Fe}/\text{H}] = -0.35$ , and isochrones in the bottom four plots have  $[\text{Fe}/\text{H}] = 0.00$ .

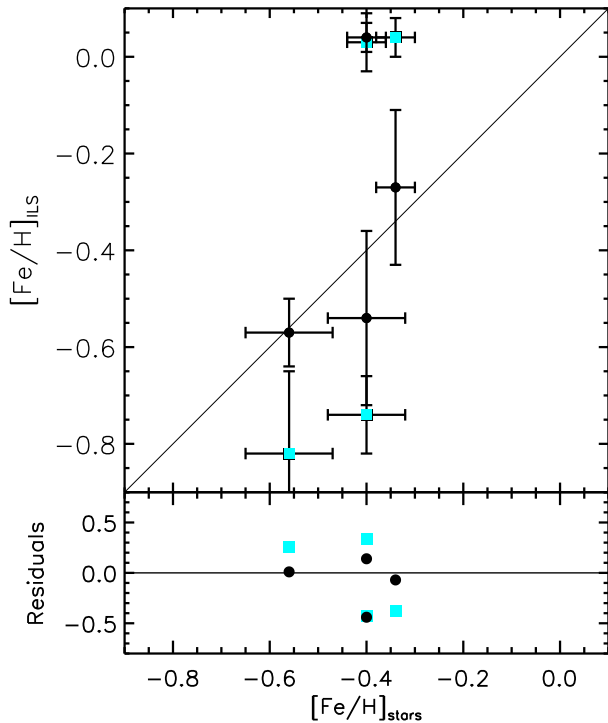


FIG. 5.— IL spectra results for CMDs without C-OVER (black circles) and with C-OVER (cyan squares) are shown against the mean abundance obtained from individual stars. The bottom panel shows the residuals from the solid black 1:1 line.

vidual stars that are analyzed in this work.

Finally, we note that clusters in the LMC have long been used to put constraints on stellar evolution and SSP models because the LMC is close enough that the stellar populations of star clusters are resolved, and the LMC contains rich clusters of a wide range in age (10's of Myrs to  $\sim 12$  Gyrs), unlike the Milky Way. This age range is a critical regime for evaluating evolutionary models, and our IL abundance analysis method can provide a new and unique way to test stellar evolution models. As this paper shows, IL analysis can be used to constrain how much C-OVER is allowable in the models. The IL analysis can also be used to compare the abundance results from stellar models computed by different groups. For these tests to be most informative, it will be necessary to expand the sample of clusters with ages  $< 3$  Gyr that have both high resolution IL and individual star abundance analyses available.

This research was supported by NSF grant AST-0507350. The authors thank the anonymous referee for helpful comments. The authors thank A. McWilliam for careful reading of the manuscript and helpful suggestions. JEC thanks D. K. Lai for helpful discussions.

#### REFERENCES

- Alonso, A., Arribas, S., & Martínez-Roger, C. 1999, *A&AS*, 140, 261
- Barmina, R., Girardi, L., & Chiosi, C. 2002, *A&A*, 385, 847
- Bernstein, R., Shtetman, S. A., Gunnels, S. M., Mochnacki, S., & Athey, A. E. 2003, in *Society of Photo-Optical Instrumentation Engineers (SPIE) Conference Series*, Vol. 4841, Society of Photo-Optical Instrumentation Engineers (SPIE) Conference Series, ed. M. Iye & A. F. M. Moorwood, 1694–1704
- Bernstein, R. A., & McWilliam, A. 2002, in *IAU Symposium*, Vol. 207, *Extragalactic Star Clusters*, ed. D. Geisler, E. K. Grebel, & D. Minniti, 739–+
- Bernstein, R. A., Prochaska, J. X., & Bures, S. 2012, in preparation
- Brocato, E., Buonanno, R., Castellani, V., & Walker, A. R. 1989, *ApJS*, 71, 25
- Brocato, E., Castellani, V., Di Carlo, E., Raimondo, G., & Walker, A. R. 2003, *AJ*, 125, 3111
- Brocato, E., Raimondo, G., Di Carlo, E., Castellani, V., Caputo, F., & Musella, I. 2004, *Mem. Soc. Astron. Italiana*, 75, 142
- Cameron, S. A. 2009, PhD thesis, University of Michigan
- Castellani, V., Degl'Innocenti, S., Marconi, M., Prada Moroni, P. G., & Sestito, P. 2003, *A&A*, 404, 645
- Castelli, F., & Kurucz, R. L. 2004, *ArXiv Astrophysics e-prints*
- Colucci, J. E. 2010, PhD thesis, University of Michigan
- Colucci, J. E., Bernstein, R. A., Cameron, S. A., & McWilliam, A. 2012, *ApJ*, 746, 29
- Colucci, J. E., Bernstein, R. A., Cameron, S., McWilliam, A., & Cohen, J. G. 2009, *ApJ*, 704, 385
- Colucci, J. E., Bernstein, R. A., Cameron, S. A., & McWilliam, A. 2011, *ApJ*, 735, 55 (C11)
- Dirsch, B., Richtler, T., Gieren, W. P., & Hilker, M. 2000, *A&A*, 360, 133
- Ferraro, F. R., Mucciarelli, A., Carretta, E., & Origlia, L. 2006, *ApJ*, 645, L33
- Freeman, K. C., Illingworth, G., & Oemler, Jr., A. 1983, *ApJ*, 272, 488
- Girardi, L., Bressan, A., Bertelli, G., & Chiosi, C. 2000, *A&AS*, 141, 371
- Gratton, R., Sneden, C., & Carretta, E. 2004, *ARA&A*, 42, 385
- Hill, V. 1999, *A&A*, 345, 430
- Hill, V., François, P., Spite, M., Primas, F., & Spite, F. 2000, *A&A*, 364, L19
- Hill, V., & Spite, M. 1999, *Ap&SS*, 265, 469
- Jasniewicz, G., & Thevenin, F. 1994, *A&A*, 282, 717
- Keller, S. C., Bessell, M. S., & Da Costa, G. S. 2000, *AJ*, 119, 1748
- McWilliam, A., & Bernstein, R. A. 2008, *ApJ*, 684, 326
- McWilliam, A., Preston, G. W., Sneden, C., & Shtetman, S. 1995, *AJ*, 109, 2736
- Meynet, G., & Maeder, A. 2000, *A&A*, 361, 101
- Mucciarelli, A., Carretta, E., Origlia, L., & Ferraro, F. R. 2008, *AJ*, 136, 375
- Mucciarelli, A., et al. 2010, *ArXiv e-prints*
- Mucciarelli, A., Ferraro, F. R., Origlia, L., & Fusi Pecci, F. 2007a, *AJ*, 133, 2053
- Mucciarelli, A., Origlia, L., & Ferraro, F. R. 2007b, *AJ*, 134, 1813
- Olszewski, E. W., Schommer, R. A., Suntzeff, N. B., & Harris, H. C. 1991, *AJ*, 101, 515
- Pietrinferni, A., Cassisi, S., Salaris, M., & Castelli, F. 2004, *ApJ*, 612, 168
- . 2006, *ApJ*, 642, 797
- Robertson, J. W. 1974, *A&AS*, 15, 261
- Sagar, R., Richtler, T., & de Boer, K. S. 1991, *A&AS*, 90, 387
- Sneden, C. A. 1973, PhD thesis, THE UNIVERSITY OF TEXAS AT AUSTIN.
- Straniero, O., Chieffi, A., & Limongi, M. 1997, *ApJ*, 490, 425
- Testa, V., Ferraro, F. R., Chieffi, A., Straniero, O., Limongi, M., & Fusi Pecci, F. 1999, *AJ*, 118, 2839
- Ventura, P., & Castellani, M. 2005, *A&A*, 430, 1035
- Will, J., Bomans, D. J., Tucholke, H., de Boer, K. S., Grebel, E. K., Richtler, T., Seggewiss, W., & Vallenari, A. 1995, *A&AS*, 112, 367

TABLE 1  
STELLAR TARGETS

Name	RA (J2000)	Dec (J2000)	Run	$T_{\text{exp}}$ (s)	S/N (pixel <sup>-1</sup> ) (at 6500 Å)	$\lambda$ (Å)	V	$(m - M)_0$	$E(B - V)$
1978-737	82.17996	-66.20839	2004 Oct	14800	99	4800-9300	17.07	18.43	0.09
1978-730	82.21058	-66.24611	2004 Oct	5800	81	4800-9300	16.85	18.43	0.09
1866-954	78.38208	-65.46264	2004 Oct	7530	95	4100-9300	15.97	18.50	0.06
1866-1653	78.43350	-65.45370	2003 Jan	7200	78	4500-7200	15.01	18.50	0.06
1866-1667	78.40430	-65.45670	2003 Jan	7200	54	4500-7200	16.15	18.50	0.06
1711-831	72.62896	-69.97525	2003 Nov	7500	118	4700-8100	14.86	18.50	0.09
1711-988	72.66138	-69.96819	2003 Nov	4000	97	4700-8100	13.92	18.50	0.09
1711-1194	72.61679	-69.95275	2003 Nov	7000	123	4700-8100	14.81	18.50	0.09
2100-b22	85.55092	-69.20206	2003 Nov	2100	115	4700-8100	13.7	18.45	0.24
2100-c2	85.48508	-69.20747	2003 Nov	2561	123	4700-8100	13.0	18.45	0.24
2100-c12	85.53642	-69.19544	2003 Nov	2100	120	4700-8100	13.8	18.45	0.24

REFERENCES. — Coordinates and magnitudes for each cluster were taken from the following catalogs: NGC 1978 Will et al. (1995), NGC 1866 Brocato et al. (1989), NGC 1711 Sagar et al. (1991), NGC 2100 Robertson (1974). Adopted distance moduli and reddening values for the clusters were taken from the following: NGC 1978 Ferraro et al. (2006), NGC 1866 Mucciarelli et al. (2010), NGC 1711 Dirsch et al. (2000), NGC 2100 Keller et al. (2000).

TABLE 2  
 LINE PARAMETERS AND STELLAR EQUIVALENT WIDTHS

Species	$\lambda$ (Å)	E.P. (eV)	log gf	EW	EW	EW	EW	EW	EW	EW	EW	EW	EW	EW
				(mÅ) 1978 737	(mÅ) 1978 730	(mÅ) 1866 954	(mÅ) 1866 1653	(mÅ) 1866 1667	(mÅ) 1711 831	(mÅ) 1711 988	(mÅ) 1711 1194	(mÅ) 2100 c2	(mÅ) 2100 c12	(mÅ) 2100 b22
Fe I	4736.783	3.211	-0.752	...	...	185.1	...	...	...	69.5	...	...	...	...
Fe I	5001.870	3.881	0.050	...	...	...	...	...	173.1	...	...	...	...	...
Fe I	5001.870	3.881	0.050	...	...	...	...	...	153.5	...	...	...	...	...
Fe I	5014.951	3.943	-0.303	...	...	148.2	...	...	...	...	...	...	...	...
Fe I	5068.771	2.940	-1.041	...	...	189.5	...	...	195.6	...	...	...	...	...
Fe I	5074.753	4.220	-0.160	...	...	150.6	...	132.0	183.6	...	...	...	...	...
Fe I	5162.281	4.178	0.020	...	141.8	184.6	...	...	...	...	...	...	...	...
Fe I	5195.480	4.220	-0.002	...	...	185.4	...	...	180.4	...	...	...	...	...
Fe I	5367.476	4.415	0.443	...	132.6	167.4	...	157.5	...	...	...	...	...	...
Fe I	5383.380	4.312	0.645	...	...	...	...	159.4	...	...	...	...	...	...
Fe I	5389.486	4.415	-0.410	...	...	...	...	99.0	...	76.6	...	...	...	...
Fe I	5389.486	4.415	-0.410	...	...	...	...	140.8	...	...	...	...	...	...
Fe I	5569.631	3.417	-0.500	...	...	193.3	...	...	...	205.4	...	...	...	...
Fe I	5576.099	3.430	-0.900	...	...	171.0	...	158.5	192.0	...	175.8	...	...	...
Fe I	5576.099	3.430	-0.900	...	...	165.2	...	147.4	177.2	...	...	...	...	...
Fe I	6151.623	2.180	-3.330	141.1	...	145.6	173.9	...	...	26.1	...	...	...	...
Fe I	6173.341	2.220	-2.863	...	...	174.2	...	142.5	190.8	42.8	...	...	...	...
Fe I	6173.341	2.220	-2.863	...	...	168.8	...	...	...	...	...	...	...	...
Fe I	6180.209	2.730	-2.628	142.8	128.4	...	172.9	126.3	166.6	...	...	...	...	...
Fe I	6180.209	2.730	-2.628	138.6	...	...	136.5	...	...	...	...	...	...	...
Fe I	6187.995	3.940	-1.673	84.9	...	83.8	120.3	99.9	85.1	24.5	...	...	136.0	158.3
Fe I	6187.995	3.940	-1.673	102.6	...	84.7	128.3	104.0	...	27.8	...	...	...	...
Fe I	6200.321	2.610	-2.386	140.2	125.7	163.0	...	...	180.7	50.0	...	...	...	240.3
Fe I	6200.321	2.610	-2.386	...	...	153.5	...	...	...	51.2	...	...	...	...
Fe I	6213.437	2.220	-2.490	...	...	192.7	...	...	195.8	70.4	...	...	...	...
Fe I	6219.287	2.200	-2.428	...	...	...	...	154.4	...	81.2	...	...	...	...
Fe I	6229.232	2.830	-2.821	123.9	...	100.5	147.1	99.8	108.0	...	...	...	...	193.4
Fe I	6240.653	2.220	-3.212	...	...	...	...	...	163.6	26.7	...	...	...	...
Fe I	6246.327	3.600	-0.796	137.9	137.8	167.6	167.4	149.7	176.2	98.8	...	...	...	...
Fe I	6265.141	2.180	-2.532	...	...	...	...	...	...	74.9	...	...	...	...
Fe I	6270.231	2.860	-2.543	130.9	117.9	...	...	...	149.7	...	...	...	...	...
Fe I	6297.799	2.220	-2.669	...	...	180.4	...	...	...	...	...	...	...	...
Fe I	6301.508	3.650	-0.701	...	133.6	176.9	...	154.9	...	...	169.6	...	...	...
Fe I	6301.508	3.650	-0.701	...	149.9	166.5	...	...	...	...	...	...	...	...
Fe I	6307.854	3.640	-3.270	35.7	...	35.2	...	37.4	27.2	...	24.8	...	...	...
Fe I	6307.854	3.640	-3.270	28.7	...	28.3	...	...	24.2	...	...	...	...	...
Fe I	6311.504	2.830	-3.153	129.0	...	88.1	...	101.4	...	...	...	...	...	192.9
Fe I	6311.504	2.830	-3.153	...	...	88.6	...	...	...	...	...	...	...	...
Fe I	6322.694	2.590	-2.438	...	...	163.6	...	154.1	187.0	58.5	167.0	...	...	...
Fe I	6330.852	4.730	-1.640	50.1	41.0	53.3	...	...	53.5	...	52.4	...	75.0	73.0
Fe I	6335.337	2.200	-2.175	...	...	...	...	...	...	89.6	...	...	...	...
Fe I	6336.830	3.690	-0.667	147.8	134.5	168.2	...	...	179.9	77.3	176.9	...	...	...
Fe I	6353.849	0.910	-6.360	74.0	85.6	...	103.4	...	...	...	...	...	149.6	147.7
Fe I	6355.035	2.840	-2.328	...	...	...	...	...	...	40.5	...	...	...	...
Fe I	6380.750	4.190	-1.366	97.5	80.7	...	128.0	...	...	34.8	90.3	...	...	154.5
Fe I	6392.538	2.280	-3.957	106.1	108.7	83.3	125.3	62.3	95.5	11.4	95.5	...	...	170.4
Fe I	6411.658	3.650	-0.646	...	...	175.0	...	...	190.9	49.6	198.7	...	...	...
Fe I	6411.658	3.650	-0.646	...	...	185.4	...	...	193.8	190.7	...	...	...	...
Fe I	6419.956	4.730	-0.183	125.0	...	108.6	137.2	101.0	...	63.0	90.0	...	...	177.1
Fe I	6475.632	2.560	-2.929	139.4	139.5	...	...	126.0	168.7	60.2	173.4	...	...	...
Fe I	6481.878	2.280	-2.985	...	...	163.4	...	...	199.0	...	196.6	...	...	...
Fe I	6498.945	0.960	-4.675	...	...	...	...	...	...	24.4	...	...	...	...
Fe I	6518.373	2.830	-2.397	144.6	...	149.0	...	123.4	165.4	...	170.2	...	...	...
Fe I	6533.940	4.540	-1.360	53.8	57.2	59.4	...	...	64.7	...	61.7	113.7	95.8	83.2
Fe I	6533.940	4.540	-1.360	59.0	59.0	60.1	...	...	...	...	...	...	...	...
Fe I	6556.806	4.790	-1.720	28.4	62.4	29.2	...	14.8	24.5	...	26.3	...	...	...
Fe I	6569.224	4.730	-0.380	134.1	...	103.4	142.4	126.2	...	...	...	...	...	...
Fe I	6571.180	4.290	-2.950	27.5	38.8	...	...	...	...	...	...	...	...	...
Fe I	6597.571	4.770	-0.970	57.8	60.7	57.3	85.9	89.5	63.3	21.6	...	115.4	120.9	...
Fe I	6608.044	2.270	-3.939	133.1	...	81.9	148.2	...	...	...	...	...	...	...
Fe I	6627.560	4.530	-1.559	53.9	42.1	58.3	69.5	45.2	...	...	...	84.5	77.6	...
Fe I	6646.966	2.600	-3.917	71.6	58.6	...	99.7	68.5	...	...	...	125.6	111.6	...
Fe I	6646.966	2.600	-3.917	...	...	...	...	...	...	...	...	...	118.8	...
Fe I	6648.121	1.010	-5.730	106.7	98.1	85.2	141.6	58.5	...	...	...	...	...	...
Fe I	6648.121	1.010	-5.730	...	...	84.7	...	...	...	...	...	...	...	...
Fe I	6653.911	4.140	-2.447	39.8	34.0	...	53.0	...	...	...	...	...	60.8	...
Fe I	6699.136	4.590	-2.117	16.3	...	23.0	...	...	23.0	...	20.7	...	...	...
Fe I	6703.576	2.760	-3.059	102.3	124.4	98.7	...	...	...	16.2	...	...	...	...
Fe I	6704.500	4.200	-2.587	22.0	...	22.1	...	12.0	27.0	...	26.7	...	...	...
Fe I	6705.105	4.610	-1.060	59.2	...	75.2	...	105.1	73.3	...	...	...	96.6	...
Fe I	6710.323	1.480	-4.807	116.3	139.0	...	...	119.2	158.2	...	159.6	...	...	...
Fe I	6713.745	4.790	-1.479	...	...	42.2	...	34.7	40.7	...	...	...	54.3	...

TABLE 2 — *Continued*

Species	$\lambda$ (Å)	E.P. (eV)	log gf	EW	EW	EW	EW	EW	EW	EW	EW	EW	EW	EW	
				(mÅ) 1978 737	(mÅ) 1978 730	(mÅ) 1866 954	(mÅ) 1866 1653	(mÅ) 1866 1667	(mÅ) 1711 831	(mÅ) 1711 988	(mÅ) 1711 1194	(mÅ) 2100 c2	(mÅ) 2100 c12	(mÅ) 2100 b22	
Fe I	6715.386	4.590	-1.540	65.5	...	57.4	...	49.5	...	...	...	...	...	117.2	...
Fe I	6725.364	4.100	-2.227	49.7	...	47.1	...	44.5	51.7	...	...	...	...	91.2	...
Fe I	6726.673	4.590	-1.087	63.5	...	71.0	...	...	67.7	...	...	...	...	...	...
Fe I	6733.153	4.620	-1.479	46.0	...	51.5	...	...	50.6	...	50.2	...	...	68.5	...
Fe I	6739.524	1.560	-4.801	110.3	...	89.8	...	63.3	103.1	...	109.6	...	...	...	...
Fe I	6750.164	2.420	-2.592	...	...	173.1	...	159.0	...	50.8	200.3	...	...	...	...
Fe I	6806.856	2.730	-2.633	113.0	115.2	...	140.8	112.5	111.9	...	111.4	195.6	...	...	...
Fe I	6806.856	2.730	-2.633	...	...	...	...	125.4	...	...	...	185.4	...	...	...
Fe I	6810.267	4.590	-0.992	84.8	106.1	80.3	92.5	...	81.2	26.3	...	122.2	133.8	...	...
Fe I	6810.267	4.590	-0.992	...	...	76.2	...	...	75.0	...	...	...	...	...	...
Fe I	6820.374	4.620	-1.214	70.3	69.2	65.5	...	...	68.8	...	72.1	122.5	125.3	...	...
Fe I	6828.596	4.640	-0.843	...	...	...	...	...	...	...	...	152.7	...	...	...
Fe I	6839.835	2.560	-3.378	106.6	114.4	98.7	126.7	88.1	...	15.8	...	...	...	...	...
Fe I	6841.341	4.610	-0.733	...	...	...	...	138.4	81.7	...	...	...	...	...	...
Fe I	6842.689	4.640	-1.224	62.1	49.2	61.4	81.3	45.7	71.2	27.2	...	...	...	...	...
Fe I	6843.655	3.650	-0.863	...	...	...	...	59.3	...	...	...	...	...	...	...
Fe I	6851.652	1.600	-5.247	73.6	85.0	57.9	...	54.3	...	...	...	169.0	...	...	...
Fe I	6855.723	4.390	-1.747	56.5	65.8	...	...	40.2	...	...	...	...	...	...	...
Fe I	6858.155	4.590	-0.939	72.2	79.6	75.1	...	69.3	...	31.9	...	...	...	...	...
Fe I	6916.686	4.150	-1.359	...	...	...	...	...	...	...	134.8	...	...	...	177.2
Fe I	6960.330	4.570	-1.907	...	...	...	52.2	...	...	...	...	...	101.7	85.4	...
Fe I	6978.862	2.480	-2.465	...	...	182.0	...	...	...	...	...	...	...	...	...
Fe I	6988.533	2.400	-3.519	119.8	118.7	100.3	...	83.3	123.2	...	132.1	...	...	...	...
Fe I	7007.976	4.180	-1.929	66.8	67.1	62.4	...	38.5	67.9	...	...	...	...	...	...
Fe I	7022.957	4.190	-1.148	99.9	91.1	97.0	...	...	94.8	40.3	97.7	...	...	157.2	...
Fe I	7024.644	4.540	-1.106	107.3	102.6	...	...	...	...	...	...	...	...	...	...
Fe I	7038.220	4.220	-1.214	100.9	89.9	...	...	...	...	36.9	...	...	...	...	...
Fe I	7068.423	4.070	-1.319	141.8	...	...	...	117.2	...	28.7	...	...	...	...	...
Fe I	7071.866	4.610	-1.627	73.8	...	39.9	62.5	60.0	45.0	...	48.2	97.5	87.2	117.9	...
Fe I	7072.800	4.070	-2.767	...	...	...	...	...	...	...	...	...	93.3	...	...
Fe I	7083.394	4.910	-1.327	37.1	...	50.2	59.7	44.3	42.6	...	36.8	...	...	...	...
Fe I	7090.390	4.230	-1.109	...	...	...	...	118.2	...	36.3	...	...	...	...	...
Fe I	7132.985	4.060	-1.635	...	...	77.7	132.9	77.1	79.9	...	79.2	...	...	...	...
Fe I	7142.517	4.930	-1.017	...	...	64.9	103.7	73.9	...	...	...	...	...	...	...
Fe I	7151.464	2.480	-3.657	124.8	...	100.9	...	...	35.3	...	...	...	...	...	...
Fe I	7219.680	4.060	-1.617	77.5	99.0	80.5	...	75.9	85.2	18.1	...	136.3	127.8	...	...
Fe I	7396.526	4.990	-1.567	...	...	31.7	...	...	23.5	...	...	...	...	...	...
Fe I	7396.526	4.990	-1.567	...	...	25.9	...	...	...	...	...	...	...	...	...
Fe I	7411.162	4.280	-0.287	137.7	138.1	161.8	...	...	197.4	85.0	...	149.8	135.4	...	...
Fe I	7421.560	4.640	-1.727	37.0	33.6	37.8	...	...	34.5	...	...	...	47.3	41.2	...
Fe I	7445.758	4.260	0.053	...	...	199.2	...	...	...	...	...	...	...	...	...
Fe I	7454.004	4.190	-2.337	48.6	33.3	...	...	...	...	...	...	80.3	70.9	...	...
Fe I	7461.527	2.560	-3.507	116.5	112.0	95.9	...	...	...	...	...	...	...	...	...
Fe I	7477.595	3.880	-2.560	42.8	38.7	37.8	...	...	...	...	...	...	68.8	56.8	...
Fe I	7491.652	4.280	-1.067	...	...	103.4	...	...	...	39.9	...	...	...	...	...
Fe I	7498.535	4.140	-2.177	68.2	65.4	60.1	...	...	...	...	...	...	87.4	85.8	...
Fe I	7506.030	5.060	-1.230	48.3	40.8	...	...	...	...	...	...	107.5	98.5	...	...
Fe I	7507.273	4.410	-1.107	94.3	83.7	97.5	...	...	...	35.7	...	...	...	151.9	...
Fe I	7531.153	4.370	-0.557	117.9	139.1	120.9	...	...	134.6	62.5	...	...	...	...	...
Fe I	7540.444	2.730	-3.777	61.0	76.7	58.1	...	...	70.0	...	...	165.5	116.3	125.6	...
Fe I	7583.790	3.018	-1.885	...	...	186.4	...	...	192.8	...	...	...	...	...	...
Fe I	7710.363	4.220	-1.113	...	...	98.1	...	...	...	...	...	...	...	155.9	...
Fe I	7941.085	3.274	-2.286	...	97.9	166.4	...	...	...	...	...	...	...	...	...
Fe II	4508.288	2.856	-2.440	...	...	127.8	...	...	...	...	...	...	...	...	...
Fe II	4831.126	0.000	-4.890	...	...	...	...	158.6	...	...	...	...	...	...	...
Fe II	4833.197	2.657	-4.640	...	...	...	...	33.9	...	...	...	...	...	...	...
Fe II	4833.865	2.844	-5.110	...	...	...	...	36.9	...	...	...	...	...	...	...
Fe II	4923.927	2.891	-1.260	144.3	148.9	188.1	...	...	...	...	...	...	...	...	...
Fe II	4993.358	2.807	-3.620	88.8	...	49.7	...	...	56.3	...	...	...	...	...	...
Fe II	5036.920	3.017	-4.670	...	...	...	...	...	...	41.8	...	...	...	...	...
Fe II	5100.664	2.807	-4.170	...	...	37.6	...	...	37.3	...	...	...	...	...	...
Fe II	5120.352	2.828	-4.240	...	...	...	...	...	...	81.5	...	...	...	...	...
Fe II	5132.669	2.807	-4.080	...	...	...	...	...	...	92.5	...	...	...	...	...
Fe II	5146.127	2.828	-3.910	...	...	...	...	...	...	98.0	...	...	...	...	...
Fe II	5154.409	2.844	-4.130	57.9	...	50.3	...	...	...	...	...	...	...	...	...
Fe II	5161.184	2.856	-4.470	...	...	30.0	...	...	...	44.4	...	...	...	...	...
Fe II	5197.577	3.230	-2.220	...	...	121.9	...	...	...	44.5	...	...	...	...	...
Fe II	5234.625	3.221	-2.180	88.9	93.6	93.7	111.2	127.5	...	...	...	...	...	171.6	...
Fe II	5234.625	3.221	-2.180	96.3	...	118.6	109.6	...	...	...	...	...	...	...	...
Fe II	5256.938	2.891	-4.060	...	...	41.8	...	...	...	94.6	...	...	...	...	...
Fe II	5264.812	3.230	-3.130	...	...	...	49.6	...	...	...	...	...	...	...	...
Fe II	5325.553	3.221	-3.160	44.4	...	51.1	35.8	109.6	...	...	...	...	84.4	...	...

TABLE 2 — *Continued*

Species	$\lambda$ (Å)	E.P. (eV)	log $gf$	EW	EW	EW	EW	EW	EW	EW	EW	EW	EW	EW
				(mÅ) 1978 737	(mÅ) 1978 730	(mÅ) 1866 954	(mÅ) 1866 1653	(mÅ) 1866 1667	(mÅ) 1711 831	(mÅ) 1711 988	(mÅ) 1711 1194	(mÅ) 2100 c2	(mÅ) 2100 c12	(mÅ) 2100 b22
Fe II	5337.732	3.230	-3.720	...	29.7	53.3	49.1	36.7	...	...	...	...	66.2	58.8
Fe II	5414.073	3.221	-3.580	44.8	...	...	...	62.2	...	...	...	...	113.2	...
Fe II	5425.257	3.199	-3.220	40.9	34.3	...	42.1	50.8	42.4	...	...	99.5	55.8	55.5
Fe II	5525.125	3.267	-3.970	...	30.1	19.6	28.0	...	...	52.8	...	...	57.7	44.9
Fe II	5591.368	3.267	-4.440	...	...	...	...	...	...	29.6	10.3	...	30.2	...
Fe II	5591.368	3.267	-4.440	...	...	...	...	...	...	27.4	17.9	...	24.2	...
Fe II	5627.497	3.387	-4.100	...	...	...	...	...	...	46.4	...	...	...	...
Fe II	5813.677	5.571	-2.510	...	...	...	...	...	...	18.4	...	...	...	...
Fe II	5991.376	3.153	-3.540	35.3	37.0	...	...	...	...	...	37.2	...	63.4	...
Fe II	6084.111	3.199	-3.790	20.9	23.7	31.0	...	55.2	29.5	82.2	...	91.2	...	41.0
Fe II	6113.322	3.221	-4.140	...	...	24.0	...	54.3	...	56.2	...	...	...	...
Fe II	6147.741	3.889	-2.690	...	...	...	...	103.2	...	...	...	...	...	...
Fe II	6149.258	3.889	-2.690	50.3	...	42.2	54.5	...	...	87.0	...	...	...	...
Fe II	6238.392	3.889	-2.600	50.7	...	56.7	79.3	...	...	...	...	...	...	...
Fe II	6369.462	2.891	-4.110	35.1	30.0	33.8	...	...	...	82.3	...	...	...	...
Fe II	6383.722	5.553	-2.240	...	...	...	...	...	...	36.2	...	...	...	...
Fe II	6432.680	2.891	-3.570	50.5	...	58.6	...	...	53.6	...	46.2	119.2	84.1	73.9
Fe II	6442.955	5.549	-2.440	...	...	...	...	...	...	25.2	...	...	...	...
Fe II	6456.383	3.903	-2.050	50.1	39.3	64.7	...	...	56.4	...	48.8	...	...	88.5
Fe II	6516.080	2.891	-3.310	80.2	...	73.5	...	...	...	...	...	...	102.6	127.5
Fe II	6517.018	5.585	-2.730	...	...	...	...	...	...	16.4	...	...	...	...
Fe II	7222.394	3.889	-3.260	...	20.6	...	...	...	...	73.8	...	...	...	...
Fe II	7310.216	3.889	-3.370	28.7	...	68.9	...	...	...	66.7	12.4	...	...	...
Fe II	7320.654	3.892	-3.230	96.4	...	...	...	...	...	85.4	...	...	...	...
Fe II	7449.335	3.889	-3.270	...	...	...	...	...	...	68.7	...	...	...	...
Fe II	7479.693	3.892	-3.610	...	...	...	...	...	...	43.6	...	...	...	...
Fe II	7711.724	3.903	-2.500	...	...	...	...	...	...	...	...	...	70.6	71.1

NOTE. — Lines listed twice correspond to those measured in adjacent orders with overlapping wavelength coverage. Log  $gf$  values are taken from C11 and references therein.

TABLE 3  
ABUNDANCE COMPARISON

Cluster	With C-OVER (C11a)		Without C-OVER (This Work)	
	Age (Gyrs)	[Fe/H]	Age (Gyrs)	[Fe/H]
NGC 1718	1.0–2.5	$-0.64 \pm 0.25$	1.0–2.5	$-0.70 \pm 0.03$
NGC 1978	1.5–2.5	$-0.74 \pm 0.08$	1.0–3.0	$-0.54 \pm 0.18$
NGC 1866	0.1–0.3	$+0.04 \pm 0.04$	0.1–0.5	$-0.27 \pm 0.20$
NGC 1711	0.06–0.30	$-0.82 \pm 0.17$	0.06–0.10	$-0.57 \pm 0.07$
NGC 2100	<0.04	$< -0.03 \pm 0.06$	<0.04	$-0.40 < [\text{Fe}/\text{H}] < +0.03$

NOTE. — Note that the IL abundances for NGC 1718 are shown for completeness, and that these results are not used in §4 because we do not have a sample of individual stars in this cluster.

TABLE 4  
FINAL STELLAR PARAMETERS AND FE ABUNDANCE RESULTS

Name	$M_V^a$	$B - V^a$	$T_{eff}$ (K)	$\log(g)$	$\xi$ ( $\text{kms}^{-1}$ )	$[\text{Fe}/\text{H}]_{\text{I}}^b$	$N_{\text{FeI}}$	$[\text{Fe}/\text{H}]_{\text{II}}^b$	$N_{\text{FeII}}$	$v_r$ ( $\text{kms}^{-1}$ )
1978-737	-1.64	1.56	4079	0.96	1.70	-0.46±0.24	69	-0.43±0.34	17	290.1±0.1
1978-730	-1.86	1.68	3902	0.62	1.35	-0.34±0.28	49	-0.31±0.24	9	292.9±0.1
1866-954	-2.64	1.15	4400	1.84	1.90	-0.39±0.15	93	-0.34±0.19	24	300.6±0.1
1866-1653	-3.60	1.43	4157	0.74	2.30	-0.31±0.19	26	-0.62±0.40	8	302.7±0.3
1866-1667	-2.46	0.96	4802	1.71	1.95	-0.33±0.24	56	-0.47±0.41	13	301.1±0.1
1711-831	-3.92	1.40	4050	0.92	2.15	-0.62±0.23	59	-0.69±0.11	7	244.1±0.1
1711-1194	-3.97	1.42	4070	0.80	2.10	-0.61±0.24	31	-0.66±0.21	6	247.0±0.1
1711-988	-4.86	0.50	5850	1.54	1.75	-0.46±0.11	39	-0.24±0.16	26	241.4±0.1
2100-b22	-5.50	1.51	3885	0.17	3.30	-0.43±0.22	20	-0.40±0.24	10	253.5±0.1
2100-c2	-6.20	1.38	4150	0.05	2.20	-0.03±0.22	17	-0.07±0.20	3	242.2±0.1
2100-c12	-5.40	1.49	4000	0.24	3.30	-0.37±0.24	27	-0.42±0.31	12	247.2±0.1

<sup>a</sup> V magnitudes and  $B - V$  colors have been distance and reddening corrected with the  $(m - M)$  and  $E(B - V)$  values in Table 1.

<sup>b</sup> The quoted uncertainty for Fe I and Fe II abundances is the standard deviation in the abundance of all of the measured lines of each species,  $\sigma_{\text{Fe}}$ .

TABLE 5  
STELLAR PARAMETER COMPARISON

Name	$T_{\text{phot}}$ (K)	Initial Photometric Parameters				Spectroscopic, $\log g$ constant				Spectroscopic, $\log g$ adjusted		
		$\log(g_{\text{phot}})$	$\xi_{\text{phot}}$ ( $\text{kms}^{-1}$ )	$[\text{Fe}/\text{H}]_{\text{I, phot}}$	$[\text{Fe}/\text{H}]_{\text{II, phot}}$	$T_{\text{Ex}}$ (K)	$\xi_{\text{Spec}}$ ( $\text{kms}^{-1}$ )	$[\text{Fe}/\text{H}]_{\text{I, spec1}}$	$[\text{Fe}/\text{H}]_{\text{II, spec1}}$	$\log(g_{\text{Ion}})$	$[\text{Fe}/\text{H}]_{\text{I, spec2}}$	$[\text{Fe}/\text{H}]_{\text{II, spec2}}$
1978-737	3879	0.96	1.74	-0.43	-0.09	4079	1.70	-0.46	-0.43	...	...	...
1978-730	3742	0.72	1.79	-0.55	-0.16	3902	1.35	-0.34	-0.25	0.62	-0.34	-0.31
1866-954	4469	1.44	1.64	-0.29	-0.54	4400	1.90	-0.45	-0.58	1.84	-0.39	-0.34
1866-1653	4057	0.74	1.79	-0.08	-0.32	4157	2.30	-0.31	-0.62	...	...	...
1866-1667	4802	1.71	1.58	-0.16	-0.33	4802	1.95	-0.33	-0.47	...	...	...
1711-831	4097	0.92	1.74	-0.36	-0.54	4050	2.15	-0.62	-0.69	...	...	...
1711-1194	4070	0.8	1.76	-0.37	-0.47	4070	2.10	-0.61	-0.66	...	...	...
1711-988	6012	1.54	1.62	-0.35	-0.19	5850	1.75	-0.48	-0.24	...	...	...
2100-b22	3971	0.17	1.91	+0.18	-0.17	3885	3.30	-0.43	-0.40	...	...	...
2100-c2	4249	0.05	1.93	+0.15	-0.10	4150	2.20	-0.03	-0.07	...	...	...
2100-c12	3997	0.24	1.89	+0.05	+0.03	4000	3.30	-0.37	-0.42	...	...	...

TABLE 6  
UNCERTAINTIES IN FE ABUNDANCE WITH STELLAR PARAMETERS

Name	$T_{eff}$ (+150 K)	$\log g$ (-0.5 dex)	$\xi$ (+0.3 $\text{kms}^{-1}$ )	$[\text{M}/\text{H}]$ (+0.3 dex)
1978-737	+0.02	-0.10	-0.11	+0.07
1978-730	-0.09	-0.18	-0.10	+0.00
1866-954	+0.04	-0.07	-0.12	+0.05
1866-1653	+0.04	-0.07	-0.06	+0.07
1866-1667	+0.13	+0.02	-0.10	+0.01
1711-831	-0.02	-0.10	-0.12	+0.07
1711-988	+0.10	+0.03	-0.05	+0.00
1711-1194	+0.02	-0.11	-0.13	+0.07
2100-b22	-0.05	...	-0.24	-0.07
2100-c2	-0.05	...	-0.18	+0.04
2100-c12	+0.02	-0.09	-0.04	+0.02

TABLE 7  
COMPARISON OF MEAN CLUSTER ABUNDANCES

Cluster	ILS This Work	Stars This Work	Stars Other Authors	Ref
NGC 1978	$-0.54 \pm 0.18$	$-0.40 \pm 0.08$	$-0.38 \pm 0.12$	1
			$-0.96 \pm 0.20$	2
NGC 1866	$-0.27 \pm 0.20$	$-0.34 \pm 0.04$	$-0.50 \pm 0.10$	2
			$-0.43 \pm 0.04$	3
NGC 1711	$-0.57 \pm 0.07$	$-0.56 \pm 0.09$	$-0.57 \pm 0.17^b$	4
NGC 2100	$-0.40 < [\text{Fe}/\text{H}] < +0.03$	$-0.40 \pm 0.04$	$-0.32 \pm 0.03$	5
			$-0.57 \pm 0.06$	6

REFERENCES. — 1. Mucciarelli et al. (2008), 2. Hill et al. (2000), 3. Mucciarelli et al. (2010), 4. Dirsch et al. (2000), 5. Jasniewicz & Thevenin (1994), 6. Hill & Spite (1999)

<sup>a</sup> The uncertainties listed for the cluster metallicities in our work are obtained from the standard deviation in the individual stellar abundances from Table 4.

<sup>b</sup> Note that this value is derived from Strömgren photometry, while all other stellar results from the literature are derived from high resolution spectra.